

POMDP Manipulation Planning under Object Composition Uncertainty

Joni Pajarinen^{1,2}, Jens Lundell¹ and Ville Kyrki¹

Abstract—Manipulating unknown objects in a cluttered environment is difficult because segmentation of the scene into objects, that is, object composition is uncertain. Due to this uncertainty, earlier work has concentrated on either identifying the “best” object composition and deciding on manipulation actions accordingly, or, tried to greedily gather information about the “best” object composition. Contrary to earlier work, we 1) utilize different possible object compositions in planning, 2) take advantage of object composition information provided by robot actions, 3) take into account the effect of different competing object hypotheses on the actual task to be performed. We cast the manipulation planning problem as a partially observable Markov decision process (POMDP) which plans over possible hypotheses of object compositions. The POMDP model chooses the action that maximizes the long-term expected task specific utility, and while doing so, considers the value of informative actions and the effect of different object hypotheses on the completion of the task. In simulations and in experiments with an RGB-D sensor, a Kinova Jaco and a Franka Emika Panda robot arm, a probabilistic approach outperforms an approach that only considers the most likely object composition and long term planning outperforms greedy decision making.

Index Terms—POMDP, image segmentation, robotic manipulation, task planning, grasping

I. INTRODUCTION

Service robots in domestic environments need the ability to manipulate objects without good prior models in order to cope with the variability of such environments. This need is usually approached by attempting to model the objects on-line using sensors based on stereopsis or structured light. When multiple measurements can be acquired around an isolated object, this approach works quite satisfactorily as the generated 3-D models can often be used for successful manipulation.

In cluttered scenes with multiple unknown objects, the segmentation of objects, also known as object discovery in perception research, becomes a major problem. Typically, the problem is to decide which of the segments in an oversegmented scene belong to the same object. This is challenging especially because objects can be partially occluded by others. A promising approach towards solving object discovery is interactive perception [1], where the object configuration is examined actively, typically by manipulating the objects and observing the results. Another line of work is to use learned

priors to find the most likely object composition. Despite the recent advances, manipulation of unknown objects in cluttered environments is still an open problem.

This paper proposes a solution to manipulation planning, which plans over hypotheses of possible object compositions (segmentations) instead of trying to determine a single best hypothesis. For estimating the distribution of object compositions we propose a Markov chain Monte Carlo (MCMC) procedure that produces approximately exact, independent samples from the distribution. The approach combines earlier ideas of interactive perception and learned composition priors in a planning under uncertainty framework. The manipulation planning problem is cast as a partially observable Markov decision process (POMDP), which integrates active exploration and planning. This allows us to take advantage of information provided by robot actions, plan actions under object composition uncertainty into the future, and thus tackle manipulation in challenging environments. In contrast to earlier work, our approach 1) utilizes different possible object compositions in decision making, 2) takes into account the effect of competing hypotheses on the goal task, and 3) actively explores the hypothesis space if that benefits the task. This journal article extends our earlier conference papers [2] and [3] (i) by combining the MCMC procedure for belief estimation in [2] with the POMDP planning in [3]; (ii) by including fully hidden objects into the POMDP model by taking advantage of hidden volume information; (iii) by a high volume of simulations for statistically significant evaluations; (iv) new results using a Franka Panda robotic arm verifying the general applicability of the approach.

This paper begins by surveying work related to object discovery, interactive perception and planning under uncertainty in Section II. Our framework of manipulation planning over object compositions is then introduced in Section III. Section IV proposes our approach for estimating the distribution over object hypotheses. The state space of hypotheses is then used for manipulation planning as described in Section V. Experiments with two different physical robot arms and an RGB-D sensor presented in Section VI demonstrate that the proposed approach is able to integrate perception to the manipulation task and that the use of multiple hypotheses improves system performance when compared to considering only the most likely hypotheses. Section VII concludes the paper.

II. RELATED WORK

Our work focuses on manipulation under object composition uncertainty. Below, we discuss related work w.r.t. image

This work was supported by the Academy of Finland, decision 271394 and German Research Foundation (DFG) project PA 3179/1-1 (ROBOLEAP).

¹J. Pajarinen, J. Lundell and V. Kyrki are with the Department of Electrical Engineering and Automation, Aalto University, Finland. ²J. Pajarinen is with Intelligent Autonomous Systems, TU Darmstadt, Germany.

E-mail: Joni.Pajarinen@aalto.fi, Jens.Lundell@aalto.fi, Ville.Kyrki@aalto.fi

segmentation and object discovery since we construct object hypotheses from RGB-D data, active and interactive perception since our approach also gathers information actively when needed, grasping unknown objects, and manipulation under uncertainty.

Image segmentation. Image segmentation is a widely and actively studied research field [4]–[8]. Most of the earlier work concentrates on segmenting grey and color 2D images [4], [5], but with the introduction of new cheap 3D-sensors such as Microsoft’s Kinect or Intel’s RealSense, research on segmenting 3D images has gained in popularity [8]–[13]. The 3D information from these sensors are especially useful for robotics tasks including grasping and manipulation [13]–[17]. However, all of these methods consider only point estimates of the segmentation which, in case of poor segments, can lead to unsuccessful grasps [13].

To mitigate the influence of wrong segmentations, related works have thus focused on utilizing a probability distribution over segmentations [18], [19] or considering many segmentation hypotheses [20]. By treating the problem as such it is possible to use robots to gather information about the most likely segmentation through exploratory actions such as poking objects [19], [20]. In this work we also treat the problem probabilistically but instead of considering only distributions over segmentations we model the complete probability distribution over object compositions and use this information for downstream decision making tasks.

A common technique for finding the best object composition is through graph cuts [6], [8], [21]. In this paper, we estimate the probability distribution over object compositions using a Markov chain Monte Carlo (MCMC) procedure. Prior work on applying MCMC to find a single best segmentation exists; for example, in the task of segmenting humans from video frames using human shape models [22], or for segmenting 2D images [23]. Due to the inherent ambiguity in segmentation the authors also present in [23] a technique for selecting a fixed amount of distinct 2D segmentations, instead of only the most likely segmentation.

Object discovery. Scene segmentation is a classic problem in computer vision tightly coupled to object recognition [24], [25] so that it can be argued that the segmentation problem does not have unique solutions if the objects are not known. Nevertheless, there is a need to discover objects from scenes even when the objects are not known in advance. Recent works in the area are based on learning to detect objects based on synthetic training data [12], or often based on learning general models used to recognize object classes from segments (e.g. segment labeling in [26]), to detect segments based on their “objectness” [27], or to choose which segments belong to a single object [8], [11]. Our work follows the line of work of [8], [11] but instead of trying to find a single optimal composition as in [8], [11], [12], considers the distribution of possible compositions.

Active and interactive perception. Instead of a passive approach object discovery can be approached from the point of view of active perception [28]. Gaze control and foveation, which are purely perceptual processes, have been proposed for object discovery [29]. Furthermore, interactive perception [1]

has been proposed as a promising solution for object discovery with the goal of singulating [30], clearing [20], or segmenting [31] a pile of objects. These approaches use poking or pushing actions to estimate the object composition. This paper follows the interactive perception paradigm but in contrast to the works above, integrates the perception with goal-directed planning so that perceptual actions are only used when they are expected to support the task goal.

Grasping unknown objects. Grasping unknown objects has got significant attention in the research community, especially after Saxena’s work [32] which proposed the use of machine learning for planning good grasps. Since then, many new data-driven methods have arisen [14]–[16], [33]–[36]. Out of these the most influential works, *e.g.*, DexNet [16], [36] and 6-DOF GraspNet [15], are based on deep-learning and propose grasps directly from raw sensor readings such as depth-images or point-clouds. In order to reach a high grasp success rate grasps are often constrained to top-down and to 4 degrees of freedom [14], [16], [34]. In this work we also consider top-down grasps but, instead of using a data-driven method, we align the robot hand according to the principal axes of the point-cloud. In addition, we consider grasping as a component for both informative and goal-directed actions; hence, even failed grasps give valuable information about object composition that is used for planning future grasps.

Manipulation planning under uncertainty. In planning manipulation actions under uncertainty, such as planning where to grasp an object, classical deterministic planning can be used to reduce uncertainty. For example, Dogar et al. [37] plan pre-grasp pushing actions that collapse pose uncertainty of a target before executing a grasping action. This type of approach is usually only available for completely known objects.

When faced with limited knowledge, POMDP-like approaches can be used to plan over a distribution of states. Hsiao et al. [38] proposed the partitioning of a one-dimensional configuration space to yield a discrete POMDP which can be solved for an optimal policy. In planning grasp locations, the state-of-the-art includes probabilistic approaches with a short time horizon. The goal can be formulated either as positioning the robot accurately as in [39] or maximizing the probability of a successful grasp as in [40]. The short-term planning can also be extended to include information gathering actions [41].

In POMDP based approaches for multi-object manipulation, Monso et al. [42] use a POMDP definition designed specifically for clothes separation. In contrast to [42], this paper does not assume that each object is uniform in color, but instead, complex multi-colored and textured objects are considered for object discovery. Moreover, the state space model of [42] is clothes separation specific, modeling the number of clothes in different areas. Our approach reasons about objects directly.

Li et al. [43] formulate emptying a refrigerator as a POMDP. Li et al. [43] do not explicitly model a probability distribution over object hypotheses but assume a priori six different types of known objects and perfect segmentation. Xiao et al. [44] tackle object search using a POMDP model that also considers fully occluded objects. Xiao et al. [44] assume perfect object composition segmentation with some uncertainty in object

locations. Moreover, Xiao et al. [44] assume that the number and models of objects are known in advance and use this information for finding hidden objects. In contrast to [43], [44], our approach does not assume any information on object models or number of objects. Instead, we plan manipulation actions based on a probability distribution of object compositions.

III. MANIPULATING OBJECT COMPOSITIONS

We consider the scenario of a robot manipulating unknown objects based on RGB-D data. The manipulation goal is defined in terms of simple features that can be observed incompletely from the point clouds. For example, the goal could be to move all objects with a certain color to a particular location. Manipulating unknown objects is difficult because even if RGB-D data is available, the robot does not know in advance the shape or color of the objects. Thus, the robot has to guess which parts of the point cloud belong to the same object. Occlusion and noisy sensor readings make this task hard. Attempting to segment individual objects from the point cloud typically results in oversegmentation, which leads to the problem of deciding which segment belongs to which object, in other words, forming *object hypotheses*.

In previous works such as [45], the choice of an action is based on the most probable hypothesis of object composition. The shortcoming of this approach is that it does not take into account the long term effects of uncertainty or the value of information gathering actions. Instead, we propose to choose the action that maximizes long term reward over the current and future distribution of possible object compositions. By considering a temporally evolving system, the robot can infer from past grasp attempts the likelihood of object hypotheses.

Fig. 1 shows an overview of the proposed approach. At each time step we capture an RGB-D image by a vision sensor such as a Microsoft Kinect and oversegment the RGB-D image. Further, using Markov chain Monte Carlo we generate a probability distribution over possible object compositions where each composition consists of segment patches while taking into account previous manipulation outcomes. We perform long-term planning over possible future object composition distributions using a POMDP model. Finally, the best POMDP action is executed on the robot. Before going into belief estimation and manipulation planning details, we describe first how to model robotic manipulation as a POMDP.

A. Robotic manipulation as a partially observable Markov decision process (POMDP)

A POMDP defines optimal behavior for an agent in an uncertain world with noisy, partial measurements, when the stochastic world model is accurate and when the agent's goal has been defined precisely. Previously, POMDPs have yielded good results in robotic applications such as navigation [46], autonomous driving [47], human-robot interaction [48] and manipulation [38], [42]–[44], [49]. We utilize a POMDP because it takes uncertainty in action effects and observations into account. Moreover, a POMDP assigns the correct long-term value to informative actions which are needed when exploring object hypotheses.

The temporal model of a POMDP is defined by the transition probability $P(s'|s, a)$ from state s to the next time step state s' , when action a is executed, and the probability $P(o|s', a)$ of observing o , when action a was executed and the world moved to the state s' . A real-valued reward $R(s, a)$ for executing action a in state s encodes the objective. An optimal policy π maximizes the expected reward $E[\sum_{t=0}^{T-1} R(s(t), a(t)) | \pi, b_0]$ over T time steps, where b_0 denotes the initial *belief*, a probability distribution over world states. At each time step, the agent decides on an action a based on its current belief. In principle, the belief can be kept up-to-date given an accurate temporal model. However, because an accurate model is in practice not available, we instead estimate the belief at each time step from current visual sensor data and past history, and use the *online* POMDP method called particle based policy graph improvement algorithm (PPGI) introduced in [49] (the technical report [50] provides further details) to compute a new policy. To cope with a huge state space, PPGI uses a state particle representation for the belief $b(s)$.

Our POMDP model uses a probability distribution over possible object hypotheses. Grasping actions occur in the space of object hypotheses. Shortly, the probability of successfully grasping a hypothetical object, and observing its attributes (for example color), depend on how occluded the object is [49]. Moreover, we assume that a previously failed grasp can not succeed unless the occlusion on the grasped object changes. Formally, the POMDP state $s = (s_1, s_2, \dots, s_N)$ is a combination of object states $s_i = (s_i^{\text{loc}}, s_i^{\text{attr}}, s_i^{\text{hist}})$ where s_i^{loc} is the semantic location such as “on top of the table” or “in a box”, s_i^{attr} attributes such as object color, and s_i^{hist} historical information for object i . The number of objects N and the objects s_i themselves differ between different POMDP states since we model a variety of object hypotheses as discussed in more detail next.

IV. BELIEF ESTIMATION

The belief consists of state particles and their probabilities. Here, instead of objects, each state consists of a set of *object hypotheses* called an *object composition*. An object hypothesis consists of a set of segments, where every segment is connected either directly or in-directly to each other. The segments are not connected to segments outside this set. Two segments can be directly connected if they occlude each other or if another object occludes both (the direct connection is then behind this occluding object).

The probability of a sampled state is proportional to the probability of the related object composition to exist. The probability for an object composition to exist depends on the history of successful and failed grasps. The key insight is that previously performed grasps must have failed for an object hypothesis, otherwise the object would have been moved. Furthermore, a grasp can only succeed for an incorrect hypothesis, when the incorrect hypothesis is part of a hypothesis, for which the grasp succeeds.

To estimate the belief, we segment the observed point cloud and compute the connectedness probability for each segment pair. Based on these probabilities, and whether segments can

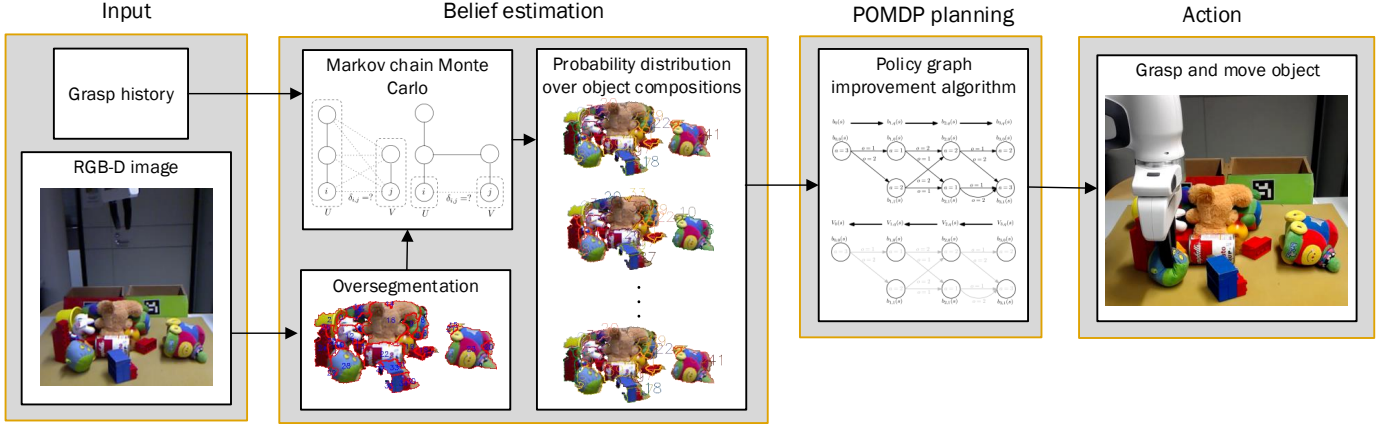


Fig. 1. Overview of the proposed approach. At each time instant the robot obtains and oversegments RGB-D scene data. From pair-wise segment probabilities of belonging to the same object we generate a probability distribution over possible object compositions. We condition the probability distribution on past grasp successes and failures (Section IV). The robot uses a POMDP to select the best long-term manipulation action for the current object distribution (Section V) and executes the action. For segmenting RGB-D data and estimating probabilities for segment pairs, we use [8].

be directly connected, we define a Markov chain which converges to a distribution over object compositions. We sample object compositions from this Markov chain after a burn-in period. A belief state corresponds to a sampled object composition with sampled object attributes. The probability of the belief state is set proportional to the probability of the sampled object composition, which is computed (for uniform priors) as the probability of the observation/action history conditional on the object composition. This means that the belief over object compositions is shaped by past events: for example, if the robot fails to grasp an object hypothesis, which should be easy to grasp when the object hypothesis is correct, then the hypothesis is likely incorrect, and the belief will reflect this. Fig. 2 illustrates how grasp successes and failures influence the probability distribution over object compositions. Next, we will discuss how to sample object compositions and then show how to estimate the conditional probability of an object composition given past events.

A. Markov chain sampling of object compositions

To generate object compositions in a computationally efficient way, we first segment the image into pixel patches or segments as shown in Fig. 1, and then combine the segments into object compositions which consist of object hypotheses. Previous work on segmenting an image and then combining the segments into a single object composition immediately [8], or through interaction [18], [19], exists. We instead maintain a probability distribution over object compositions and make decisions based on the probability distribution.

More formally, denote with $\delta_{i,j}$ whether segments i and j are directly connected: $\delta_{i,j} = 1$ and $\delta_{i,j} = 0$ denote direct and no direct connection, respectively. Direct connection means segments are assumed physically connected. Denote with δ all possible direct connections. Denote with $\mathbf{h} = (h_1, \dots, h_N) \in \mathcal{H}$ an object composition, where h_k is an object hypothesis and \mathcal{H} the space of object compositions. An object hypothesis h_k is a set of segment indices where all index pairs $i \in h_k$, $j \in h_k$ are connected either directly or indirectly through other

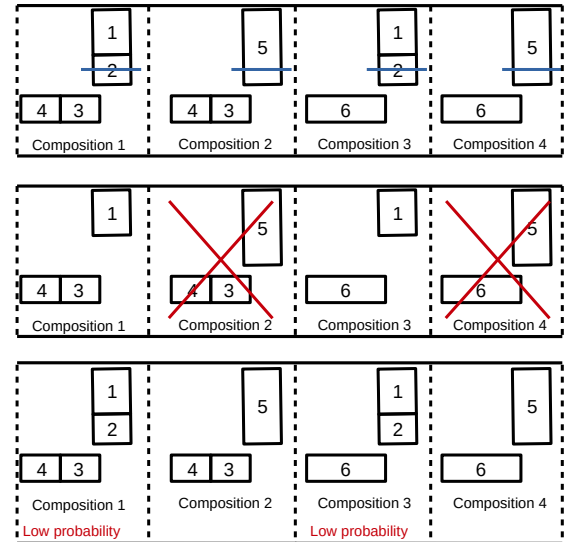


Fig. 2. Illustration of conditioning on grasp outcome. Here the probability distribution over object compositions consists of four possible compositions with six possible objects. **(Top)** The robot executes blue grasp that grasps object 2. **(Middle)** The grasp succeeds and object 2 is removed. Compositions 2 and 4 which did not contain object 2 conflict with reality and are eliminated. **(Bottom)** The grasp fails either due to object 2 not existing or a bad grasp. Therefore, probability of object compositions that contain object 2 decreases.

segments, denoted with $c_{i,j}(h_k) = 1$ for all index pairs $i \in h_k$, $j \in h_k$ and $c_{i,j}(h_k) = 0$ otherwise. Note that our sampling procedure in Algorithm 1 in Section IV-B uses direct and indirect connections to estimate the probability of a segment pair connection.

In the worst case, the dimensionality of $|\mathcal{H}|$ is $2^{N^2/2}$ w.r.t. the number of segments N . In practice, $|\mathcal{H}|$ is usually lower since segments with only “air” between them cannot be directly connected. Often, in real-world scenes, $|\mathcal{H}|$ is a product of the dimensionality of disconnected groups of segments $\prod_i 2^{N_i^2/2}$, where N_i is the number of segments in a segment group. For exact computation this is still intractable, and therefore we use an approximate particle representation for

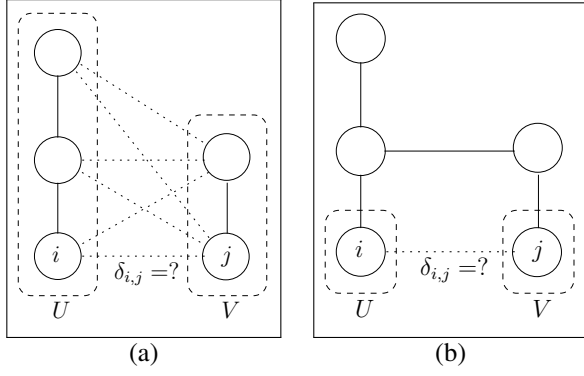


Fig. 3. Effect of indirect connections on the connection probability between segments i and j . A circle denotes a segment and a solid line denotes a connection between segments. Dotted lines denote which connection probabilities are used for sampling the connection between i and j . U and V denote the sets of segments directly or indirectly connected to i and j , respectively. (a) Because i and j are not indirectly connected we have to consider the connection probabilities between segments that will become part of the same object, that is, we have to take into account the connection probabilities between all segments in the sets U and V . (b) Because i and j are already indirectly connected we consider only the probability of the direct connection between i and j .

the probability distribution over object compositions: $P(\mathbf{h}) = \sum_i w_i \mathbf{h}_i$, where $\sum_i w_i = 1$ and $w_i \geq 0 \forall i$.

B. Markov chain Monte Carlo

In order to generate the particle based probability distribution over object compositions which can be used as a basis for decision making, we utilise Gibbs sampling (also known as Glauber dynamics) [51]–[53]. We randomly sample direct connections one connection at a time. We will first discuss how a new Markov chain state is sampled, then show that the proposed Markov chain is ergodic and converges to a unique distribution for non-deterministic connection probabilities, and finally present a sampling procedure that aims to generate exact, independent samples.

Our sampling technique for generating a new Markov chain state takes advantage of the fact that evaluating the probability for a single segment connection is fast because we only need to consider local segment connections. The sampling technique consists of two steps: 1) select randomly two segments i and j which may be directly connected, 2) sample the direct connection from the probability distribution, which is estimated by assuming the direct connection is disabled and by keeping other direct connections fixed to their current values. When i and j are indirectly connected, that is, part of the same object through some other connections, the probability for the direct connection between i and j depends only on the prior probability of i and j being part of the same object because connecting i and j would not change which object hypothesis other segments would belong to. When i and j are not already part of the same object, the probability for the direct connection depends on the probabilities between the segment sets U and V which connecting i and j would connect into the same object hypothesis. Fig. 3 illustrates this.

Algorithm 1 defines formally how to sample a new object composition \mathbf{h}^* , when given the current object composition

```

1  $\mathbf{h}^* = \text{Sample}(\mathbf{h}, w, q)$ 
   Input: Composition  $\mathbf{h}$ , random values  $w$  and  $q$ 
   Output: New composition  $\mathbf{h}^*$ 
2  $\delta_{i,j} \leftarrow$  The  $w$ th direct connection
3  $\mathbf{h}^* \leftarrow \mathbf{h}$  so that  $\delta_{i,j} = 0$ 
4  $U \leftarrow \begin{cases} i & \text{if } c_{i,j}(\mathbf{h}^*) = 1 \\ i \cup \{u | c_{i,u}(\mathbf{h}^*) = 1\} & \text{if } c_{i,j}(\mathbf{h}^*) = 0 \end{cases}$ 
5  $V \leftarrow \begin{cases} j & \text{if } c_{i,j}(\mathbf{h}^*) = 1 \\ j \cup \{v | c_{j,v}(\mathbf{h}^*) = 1\} & \text{if } c_{i,j}(\mathbf{h}^*) = 0 \end{cases}$ 
6  $P(\mathbf{h}^* | \delta_{i,j}^* = 1) \leftarrow \frac{1}{Z(U,V,\mathbf{h}^*)} \prod_{u \in U} \prod_{v \in V} P(c_{u,v}(\mathbf{h}^*) = 1)$ 
7  $P(\mathbf{h}^* | \delta_{i,j}^* = 0) \leftarrow \frac{1}{Z(U,V,\mathbf{h}^*)} \prod_{u \in U} \prod_{v \in V} P(c_{u,v}(\mathbf{h}^*) = 0)$ 
8  $P(\delta_{i,j}^* = 1 | \mathbf{h}^*) \leftarrow \frac{P(\mathbf{h}^* | \delta_{i,j}^* = 1)}{P(\mathbf{h}^* | \delta_{i,j}^* = 1) + P(\mathbf{h}^* | \delta_{i,j}^* = 0)}$ 
9  $\delta_{i,j}^* \leftarrow \begin{cases} 0 & \text{if } P(\delta_{i,j}^* = 1 | \mathbf{h}^*) \leq q \\ 1 & \text{if } P(\delta_{i,j}^* = 1 | \mathbf{h}^*) > q \end{cases}$ 

```

Algorithm 1: Sample new object composition.

\mathbf{h} , uniformly randomly selected possible direct connection index w , and finally the sampled value $q \sim \text{Uniform}(0,1)$. The algorithm first chooses the direction connection candidate using w , then on lines 4 and 5 determines the segment sets U and V which the direct connection would connect. On lines 6, 7, the algorithm computes the probability for the segment sets U and V to belong to the same object hypothesis when i and j are connected and when not. Assuming a uniform direct connection prior, line 9 computes the direct connection probability, and line 9 finally sets the direct connection on or off using q .

a) *Ergodicity of the Markov chain:* When the connection probability $P(c_{i,j})$ for any two segment patches is non-deterministic $0 < P(c_{i,j}) < 1$, the Markov chain generated by Algorithm 1 is ergodic and converges to a unique distribution. Because $P(c_{i,j})$ is non-deterministic the probabilities on lines 6, 7, and 8 are non-deterministic, and since we randomly select the direct connection to consider, Algorithm 1 enables or disables any direct connection with non-zero probability. Therefore, the Markov chain is ergodic and converges to a unique distribution in the limit. Note that due to the inherent uncertainty in segmentation the condition $0 < P(c_{i,j}) < 1$ usually applies, e.g. in the experiments in Section VI.

b) *MCMC procedure:* We would like our MCMC approach to produce independent samples from the correct distribution. Therefore, our MCMC approach first aims to get an exact sample, that is, a sample from the correct probability distribution, then continue sampling until having enough independent samples (\mathbf{H} in Algorithm 2). Algorithm 2 shows the proposed MCMC approach. Since the Markov chain state is a discrete combination of binary variables, each variable denoting whether two segments are directly connected, we base our approach on the coupling from the past (CFTP) [54] technique which aims at providing exact samples. The basic idea of CFTP is to run Markov chains starting from each possible state with the same random numbers, starting further back in time, until the chains collapse (see [54] for why). For monotone [54] and anti-monotone [55] Markov chains

```

1  $\mathbf{H} = \text{Compositions}(N_{\text{ESS}}, N_{\text{START}}, |\mathbf{H}|)$ 
   Input: ESS target  $N_{\text{ESS}}$ 
   Output: Compositions  $\mathbf{H}$ 
2  $\{\mathbf{h}_1, T\} \leftarrow \text{CFTP}(N_{\text{START}})$ 
3  $t \leftarrow 1, \mathbf{H} \leftarrow \mathbf{h}_1$ 
4 while  $((\text{ESS}_{\min}(\mathbf{H}) < N_{\text{ESS}}) \text{ AND } (T < T_{\text{MAX}}))$  do
5   while  $t < T$  do
6      $\mathbf{h}_{t+1} \leftarrow \text{Sample}(\mathbf{h}_t, w, u)$ 
7      $\mathbf{H} \leftarrow \{\mathbf{H}, \mathbf{h}_{t+1}\}$ 
8      $t \leftarrow t + 1$ 
9   end
10   $T \leftarrow 2T$ 
11 end
12  $\mathbf{H} \leftarrow \text{Prune } \mathbf{H} \text{ evenly to size } |\mathbf{H}|$ 

```

Algorithm 2: Sample a set of object compositions.

```

1  $\{\mathbf{H}_T, T\} = \text{CFTP}(N_{\text{START}})$ 
   Input: # of start compositions  $N_{\text{START}}$ 
   Output: Composition  $\mathbf{H}_T$  at time  $T$ 
2  $\mathbf{H}_{\text{INIT}} \leftarrow \{\{\mathbf{h}_1 | \delta = 1\}, \{\mathbf{h}_2 | \delta = 0\},$ 
3    $\{\mathbf{h}_3, \dots, \mathbf{h}_{N_{\text{START}}} | \delta = \text{random}\}\}$ 
4  $T \leftarrow 1$ 
5 repeat
6    $T \leftarrow 2T, \mathbf{H}_T \leftarrow \mathbf{H}_{\text{INIT}}$ 
7    $w_T, \dots, w_{T/2} \leftarrow \text{Random}$ 
8    $u_T, \dots, u_{T/2} \leftarrow \text{Random}$ 
9   for  $t \leftarrow T$  to 1 do
10     $\mathbf{H}_{T-t+1} \leftarrow \emptyset$ 
11    foreach  $\mathbf{h}_{T-t} \in \mathbf{H}_{T-t}$  do
12       $\mathbf{H}_{T-t+1} \leftarrow \mathbf{H}_{T-t+1} \cup$ 
13         $\text{Sample}(\mathbf{h}_{T-t}, w_t, u_t)$ 
14    end
15  end
16 until  $|\mathbf{H}_T| = 1$ 

```

Algorithm 3: Coupling from the past (CFTP).

only two starting states are needed. However, our chain is not monotone nor anti-monotone. Due to the large number of states we start CFTP from a limited dispersed set of states: the all connected, all disconnected, and from a fixed number of randomly selected states. We can make the collapsed sample more likely to be exact by increasing the number of starting states: when the starting states cover the whole state space the collapsed sample will be exact [54]. Algorithm 3 shows the CFTP procedure we use. In the experiments, we used 100 (N_{START} in Algorithm 2 and Algorithm 3) starting states.

After CFTP, we start the actual sampling from the collapsed sample, and double the sampling horizon until having enough independent samples. We use the minimum of the effective sample size (ESS) [56] over all possible direct connections (N_{ESS} in Algorithm 2) as a lower bound estimate for the number of independent samples. Sampling stops when the estimate for independent samples is large enough. We also use a hard limit on the number of generated samples (T_{MAX} in Algorithm 2).

C. Probability of an object composition given past events

In general, the probability of an object composition $h = (h_1, \dots, h_N)$, where h_i is a single object hypothesis, depends on the sequence of past actions and observations $\theta_t = (a(0), o(1), a(1), o(2), \dots, a(t-1), o(t))$, where t denotes the current time step. We assume uniform priors, independent object hypotheses, and independent history events:

$$P(h|\theta_t) = \prod_{i=1}^N P(h_i|\theta_t) = \prod_{i=1}^N \prod_{k=1}^t P(a(k-1), o(k)|h_i). \quad (1)$$

For object hypothesis manipulation, we maintain a history of unique executed grasps. In our model, there is no need to remember multiple identical grasps; a previously failed grasp cannot succeed again, unless the occlusion of the object, for which the grasp is optimized, changes because then the grasp also changes. The composition probability conditional on past independent grasps ($\text{grasp}_1, \dots, \text{grasp}_M$) is

$$P(h|\theta_t) = \prod_{i=1}^N \prod_{k=1}^M P(\text{grasp}_k|h_i). \quad (2)$$

D. Hallucinating hidden objects

Due to occlusion the robot does not see the complete scene: objects can hide behind other objects as shown in Fig. 4. In order to allow the robot to reason about hidden objects we allow the robot to hallucinate hidden objects into the object composition distribution. For hallucinating hidden objects, we utilize the key insight that the probability of hidden objects depends on the amount of hidden space, and, the object occupancy density of that space. Using these assumptions we transform the probability distribution over visible objects into a probability distribution over both visible and hidden objects.

Let us denote with V_{visible} visible volume and with V_{hidden} hidden volume, that is, how much workspace the robot sees and does not see, respectively. To compute hidden volume V_{hidden} , we project each visible voxel onto the workspace boundary from the origin (camera location) and estimate the volume between the rectangular visible voxel and the voxel projected onto the workspace boundary. For each segment patch, we get the hidden volume by summing over the segment voxels. Summing over all segment patches yields then the hidden volume V_{hidden} . Let us denote the average height of the visible segment patches with d , the cube floor area with A_C , and the average number of objects with n_{objects} . The minimum for n_{objects} is set to 1. We estimate the total volume of interest V_{total} for a cubical

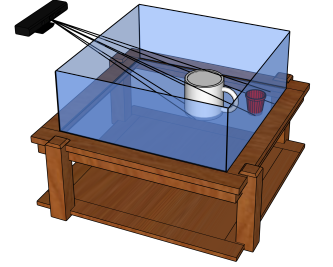


Fig. 4. Illustration of hidden objects. The transparent “glass” box denotes the workspace inside which the robot currently operates. A white cup fully occludes a red cup. To reason about hidden objects we use the insight that only a limited amount of objects can be hidden behind other objects. We assume that the probability for an object to be hidden behind another object depends on the volume hidden behind the occluding object, and, the object occupancy density.

workspace as $V_{\text{total}} = 2dA_C$. The visible volume V_{visible} is then total volume minus hidden volume: $V_{\text{visible}} = V_{\text{total}} - V_{\text{hidden}}$.

The object occupancy density is $p_{\text{objects}} = n_{\text{objects}}/V_{\text{visible}}$. For each segment patch i , we compute the expected number of hidden objects n_{objects}^i behind the patch, based on the object occupancy density p_{objects} and the patch's hidden space volume V_{hidden}^i : $n_{\text{objects}}^i = p_{\text{objects}} V_{\text{hidden}}^i$. In the experiments, although the model allows for multiple hidden objects behind an object, we assume for simplicity that there is at most one object behind an occluding object: for each state particle, a hallucinated object is sampled behind each object hypothesis according to the probability $1 - \Phi\left((1 - n_{\text{objects}}^i)/\sqrt{n_{\text{objects}}^i/4}\right)$ which corresponds to the Gaussian probability of having at least one hidden object when the mean of the Gaussian is n_{objects}^i and the standard deviation $\sqrt{n_{\text{objects}}^i/4}$. Depending on the task we can estimate probabilities for hidden object properties based on visible objects and a priori information. For example, in the object search experiments we estimate the probability for hidden objects to be red based on the average probability for redness. Now that we have discussed how to estimate the belief over object compositions we will next discuss how to plan manipulation actions using the belief.

V. MANIPULATION PLANNING

After the robot has estimated the current belief it decides on its next action based on the belief. As discussed earlier, we use a POMDP for decision making. Next, we discuss parts of our system that the POMDP requires for planning. We will discuss the actions available to the robot, how to sample a new state, how to sample an observation, and how to compute the observation probability.

A. Actions

In our problem setting, the robot may grasp an object and move it. We employ top-down grasping. For selecting the finger distance and rotation of the robot hand, we use a simple approach based on computing a vector at a narrow part of the unknown object with principal component analysis (PCA). The approach 1) projects the point cloud PC_1 of the target object hypothesis onto a plane, which is parallel to the wrist of the down-pointing robot hand, 2) makes the point density of the projected point cloud uniform to get the point cloud PC_2 , and 3) projects the centroid of PC_2 towards PC_1 along the wrist-plane normal, by the distance between the centroids of PC_1 and PC_2 , to get the grasp centroid. The approach computes the PCA decomposition of PC_2 . In PCA, the first eigenvector aligns to the largest variance in the point cloud data and the second eigenvector aligns along the second largest variance in the data. For example, for a long object, the first eigenvector could be aligned along the length of the object, and the second eigenvector along the width of the object. The approach uses the second eigenvector in order to get a narrow grasp. In more detail, the approach projects two points in opposite directions from the grasp centroid, along the computed second eigenvector, far enough. Finally, the approach selects the two points from PC_1 which are closest to the projected points, as

the two grasp contact points. In addition, the approach checks whether some part of another object hypothesis blocks the direct path up from the two grasp contact points, and if so, sets the probability of a successful grasp to zero.

1) *Restricted action set*: In order to restrict the computational load, we bound the number of possible grasps, and thus actions, by a predefined maximum number. Instead of restricting the number of possible object hypotheses, we select a subset of all hypotheses to use for grasping. Optimally, we would like to choose a set of grasps, which yields the best policy among all possible grasp sets. However, because we do not know the best policy, we settle for computing an action set that maximizes the expected grasp success probability. The grasp success probability $P_{\text{grasp prob}}(\text{SUCCESS}|h_i, A)$ defines the probability of successfully grasping and moving an object hypothesis h_i when the robot chooses the best action from the action set A . The expected grasp success probability is

$$A = \arg \max_A \sum_{h_i} P_{\text{grasp prob}}(\text{SUCCESS}|h_i, A) P(h_i), \quad (3)$$

where the number of actions is $|A|$. A can be found by an integer linear program. Unfortunately, integer linear programming is in the worst case NP-hard. As an approximation, we use a greedy approach which incrementally selects object hypothesis which increase the expected grasp success probability the most. In the experiments, the expected grasp success probability using a restricted action set remained usually close to the probability with the complete set of possible actions.

2) *Grasp success probability*: A grasp is parameterized by the distance of the finger tips, rotation of the hand, and the location of the robot wrist. The grasp success probability is the product of the *grasp quality* and an occlusion specific grasp probability. When computing grasp probabilities we take previously executed grasps into account: a failed grasp cannot succeed again, unless the occlusion of the object changes for which the grasp is optimized (when the occlusion changes the grasp usually changes also). Grasp quality is intended to capture the quality of a grasp which is optimized for another object hypothesis. Grasp quality is equal to 1 when using a grasp which was computed for the same object hypothesis that the robot tries to grasp. The grasp quality decreases when the grasp centroid moves away from the optimized grasp centroid, and becomes zero when it is outside the object. We compute the grasp quality for grasping object hypothesis X with a grasp optimized for object hypothesis Y as follows

- 1) Inside X , find starting point y_1 and end point y_2 between the grasp points of Y
- 2) If there is no y_1 or y_2 , then the grasp quality is zero because the line of grasp is outside object X
- 3) Compute centroid c_Y of y_1 and y_2
- 4) Project c_Y into the robot arm wrist plane along the plane normal
- 5) Project grasp centroid of X into the wrist plane along the plane normal to get c_X
- 6) Denote with \hat{X} the projection of X onto the wrist plane. Project a point starting from c_X through c_Y so that it is outside X and find the closest point x_1 in \hat{X}

- 7) Finally, compute the grasp quality as (distance from c_Y to x_1) / (distance from c_X to x_1), that is, the grasp quality decreases when the effective grasp centroid c_Y moves closer to the surface, away from the grasp centroid c_X optimized for X .

B. Temporal model of the world

In order to use the POMDP method in [49] for planning, we need to model the evolution of the state of the world over time. We need state transition and observation probabilities. Because probability distributions use a state particle representation, we need, in particular, a way to sample states and observations, and a way to estimate the likelihood of a state particle given an observation. Next, we discuss how to accomplish these tasks.

State sampling. As discussed earlier, a world state consists of an object composition $h = (h_1, \dots, h_N)$, and contains for each h_i a semantic object location, attributes, and history. To sample a new state for a grasp action a , select the object hypothesis h_i that has the highest grasp probability for a . Sample grasp success of a on h_i according to the grasp success probability. If the grasp fails, add the grasp to the grasp failure history of h_i . If moving an object succeeds, the semantic location of the object is changed to the destination location.

Observation sampling. After executing the grasp action, the robot observes which object was moved, and in the case of a successful move, the robot makes an observation about the attributes (color in the experiments) of a limited number of objects behind the moved object. Assuming independence between attribute observations, the observation probability is $\prod_i P(o_i|h_i)$, where o_i is the observation of h_i . As in [49], $P(o_i|h_i)$ is computed from the occlusion of h_i and the attribute instances of h_i .

Observation probability. The probability of making an observation o in state s is zero if the moved object hypothesis differs from the observed one, or if the move fails and the attribute observations do not match with previous attribute observations. Otherwise, the probability is defined by $\prod_i P(o_i|h_i)$ discussed above.

VI. EXPERIMENTS

The experiments are designed to test whether taking object composition uncertainty into account improves performance in robotic manipulation. Our hypothesis is that modeling the uncertainty explicitly is beneficial. Furthermore, we hypothesize that planning actions to accomplish a task under object composition uncertainty improves performance. The two main questions we want to answer are:

- 1) Does taking segmentation uncertainty in decision making into account increase performance?
- 2) Does multi-step planning based on a distribution over object compositions increase performance compared to greedily choosing actions?

In order to provide justified answers to these questions we compare the baseline and proposed methods in two different tasks with two different robot arms to show the generality of the methods. In the first task, the robot needs to remove objects from a table using a Kinova Jaco robotic arm. In the second

task the robot needs to search for red objects from a pile of objects in both simulation and using a Franka Panda robot arm. In the first task we focus purely on comparing decision making with and without taking segmentation uncertainty into account. In the second task, multi-step planning is needed to utilize both information gathering and task directed actions under object composition uncertainty. Therefore, we evaluate also our POMDP based planning method in the second task.

A. Segmentation, estimating grasp probabilities

In the experiments, segmentation and segment-pair probability computation is performed using the approach presented in [8]. In short, the approach assigns probabilities to segment pairs using support vector machines (SVMs) trained with RGB-D data of household items which are not in all ways similar to the toys we use in the experiments.

At each time step, the RGB-D sensor captures an RGB-D image of the scene, and the system segments the RGB-D image into patches and computes a prior probability for each patch pair to belong to the same object using the approach in [8]. In more detail, [8] groups neighbouring pixels into clusters and fits planes and B-splines onto the patches to get parametric models (see Fig. 1 for examples of segmented patches). [8] computes for each patch pair a set of features based on the texture, distance of the patches from each other, and other properties. Finally, [8] inputs the computed features into a support vector machine (SVM), trained with a labeled set of household items which differ from the items in our experiments, and scales the output into a probability indicating whether the patches belong to the same object. We use the approach of [8] to compute prior probabilities $P(c_{i,j})$ for all segment/patch pairs, where $P(c_{i,j} = 1)$ defines the prior probability for i and j to be part of the same object. Note that, in place of the segmentation approach we currently use [8], our approach can use also other approaches to over-segment and estimate patch pair probabilities.

We use $P(c_{i,j})$ in the MCMC procedure in Algorithm 2 and compute a probability distribution over object compositions (see Fig. 1 for examples). The number of MCMC samples should be chosen according to the computational budget. In the experiments, we used $|\mathbf{H}| = 2000$ samples. Because the minimum lower bound estimate ESS underestimates the real ESS it should be lower than the number of samples: we used a target ESS of $N_{\text{ESS}} = 200$, a tenth of the number of samples. The number of CFTP starting states influences the independence of the first sample w.r.t. the starting state. We used $N_{\text{START}} = 100$ CFTP starting states in the experiments. The hard limit for the number of samples generated was $T_{\text{MAX}} = 131072$.

Grasp probabilities. For grasp probability we used parameters estimated for coffee cups in [49] and we set the first color observation parameter (see [49] for details) to -0.5 and the second to -0.02 for both red and non-red observations. The models were not optimized for the particular objects because in the real-world the robot would need to be able to generalize to new objects.

B. Experiments: Clearing a Table

Fig. 5 shows the experimental setup for table clearing. In the setup, a Kinect RGB-D sensor captures images of the scene and a 6-DOF robotic Kinova Jaco arm tries to move as many toy bricks away from the table as possible. Since we do not assume any prior information in advance, including geometric or colour information, and because the bricks are in a pile, segmenting the bricks correctly is difficult. For clearly separated known objects one could possibly use standard segmentation methods.

In the experiments, we shook a box containing toy bricks shown in Fig. 5 and emptied the bricks into a specific area on a table. Fig. 6 shows the 10 random scenes for each method ordered so that the first scene produced highest utility and the last scene the lowest utility. The goal was to move a toy brick in each time step away from the table. In the application, action a specifies the object to grasp and move away. The robot is rewarded 1 for a successfully grasped and moved object and 0 otherwise.

Instead of POMDP planning we optimize in this experiment only expected immediate reward to evaluate whether utilizing a probability distribution over object compositions increases performance compared to utilizing only the best object composition found. We compare two methods. The first one, called “Best segmentation” finds first the most likely object composition \mathbf{h}^* , and then finds the action a that maximises the utility or immediate reward function $R(\mathbf{h}^*, a)$. In table clearing, “Best segmentation” tries to grasp the object which has the highest grasp success probability in the most likely object composition. The second method, called “Maximum utility”, corresponds to maximizing the expected immediate reward where the expectation is taken over possible object compositions. In table clearing, “Maximum utility” tries to grasp the object which has the highest grasp success probability weighted by the probability of the object to exist in an object composition.

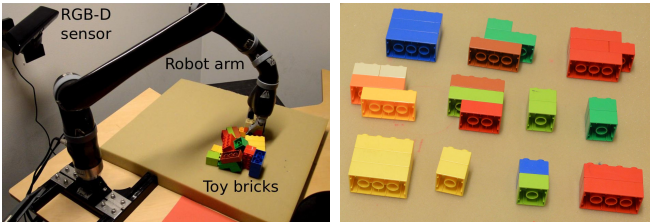


Fig. 5. In table clearing, we use an RGB-D sensor for visual input and a 6-DOF Kinova Jaco arm for grasping randomly placed toy bricks. (Left) Overall experimental setup. (Right) Toy bricks used in the experiment.

a) Table Clearing: Results & Discussion: Fig. 7 shows the number of successful moves (a maximum of six moves per scene) in 10 experimental runs for each method. One complete object movement operation, including image processing, segmenting, generating the particle based probability distribution, and moving an object, took on the average 79.9s of which our MCMC approach took 8.8s (11%). The time needed for MCMC depends on the number of particles and CFTP starting states and can be adjusted. The “Maximum utility” method performed significantly better than “Best segmentation” (the

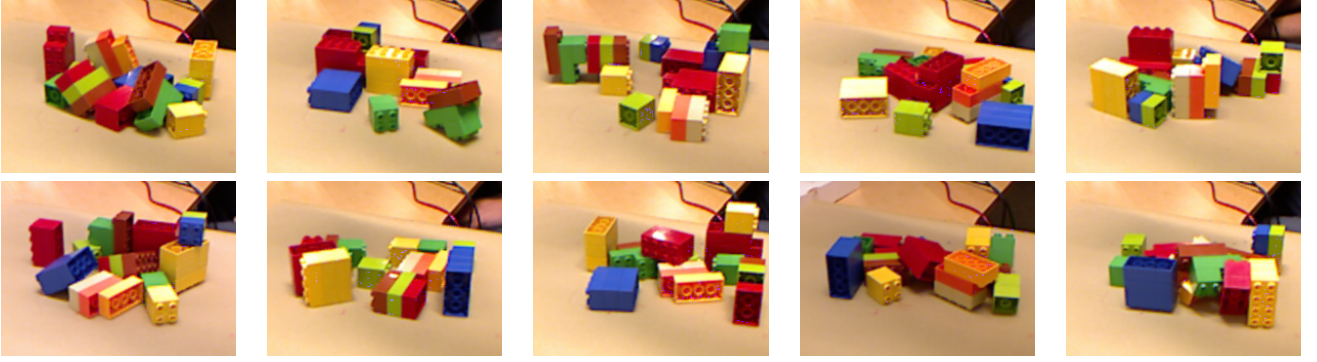
p -value was 0.014 in the Mann-Whitney U one-sided test [57]). To qualitatively compare the two methods we recorded decisions by both, although only one method operated the robot arm in each scene, that is, we ran one method and at the same time output the decisions which the other method would have made for the same object compositions. In the scenes in Fig. 6a, even though graspable objects were still available, “Maximum utility” would have finished execution early 3 times and “Best segmentation” finished early 10 times, that is, in every scene, and in the scenes in Fig. 6b “Maximum utility” finished execution early 3 times and “Best segmentation” would have finished early 23 times. The most likely composition was often missing graspable objects that were part of other object compositions. Fig. 8 shows an example of one such situation. Fig. 8a shows under-segmentation happening sometimes. In general, it is better to over-segment too heavily than under-segment but this applies to all over-segmentation approaches including the over-segmentation approach utilised by the two comparison methods. Grasps were sometimes successful even when the segmentation of the grasped object did not correspond to a real object. For example, the robot sometimes grasped the segmented top of an object and moved the complete object successfully. The robot can achieve higher performance because our utility function did not include unnecessary constraints. For applications, such as moving fragile objects, the utility function can penalize grasping an incorrectly segmented object if this could lead to dropping the object.

C. Experiments: Object Search

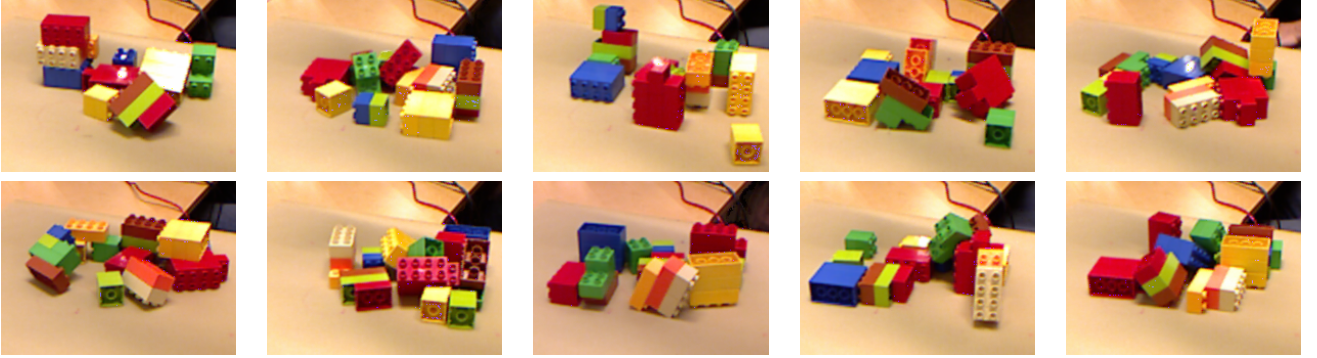
In the object search experiments, a Kinect RGB-D sensor observes objects on a table and a *Franka Emika Panda* robot arm with an attached custom parallel gripper manipulates the objects. Figure 9 shows the objects used in the experiment. We chose these objects as they differ in size, rigidness, color, and texture. In order to get diverse and unbiased scenes for each trial, we placed the objects inside a box which was shaken and emptied into the workspace of the robot. If an object ended up outside the workspace the process was repeated.

The task the robot had to solve was to find and move an unknown number of fully red objects into the red box shown in Figure 9. For every red object the robot places in the red box we increase the score (utility) by 1 and for every non-red object placed in the red box we decrease the score by 1. To remove occlusions that hinder color detection and grasping, the robot may also move objects into a green box without any direct effect on the total score, *i.e.*, we neither add nor subtract points for such an action.

Object search [44], [58] is a well known task in robotics but existing approaches do not explicitly take composition uncertainty in planning actions into account. Of recent work [58] performs object search for a pre-specified target by segmenting an image in each time step and combining the segmented image with an “occupancy distribution” that describes where the object could be hidden. We consider a more general case without a specific target object and without knowing the sizes of the objects we are searching for. [44]



(a) Random scenes in “Best segmentation” evaluations, ordered according to experimental success from best to worst



(b) Random scenes in “Maximum utility” evaluations, ordered according to experimental success from best to worst

Fig. 6. Cropped kinect RGB images of the 20 randomly generated scenes in table clearing.

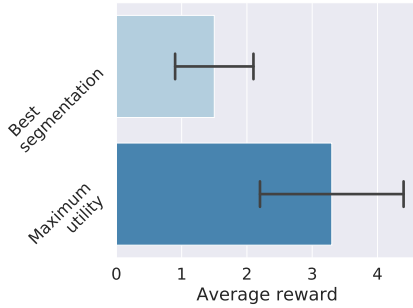


Fig. 7. Results in table clearing. The robot grasps and moves toy bricks away from the table. The bar plot shows the average number of successful moves (average reward) and the 95% confidence interval in 10 experimental runs for each method. The “Maximum utility” method performed significantly better than “Best segmentation” ($p = 0.014$ in the Mann-Whitney U one-sided test [57]).

uses a POMDP model for object search but assumes perfect object composition segmentation with some uncertainty in object locations and utilizes a priori knowledge of number and models of objects for finding hidden objects. We evaluated four different methods:

- Best grasp for objects observed red in the most likely segmentation (“Best segmentation”)
- Grasp for the highest expected immediate reward (“Maximum utility”)
- POMDP multi-step planning without hallucinating hidden

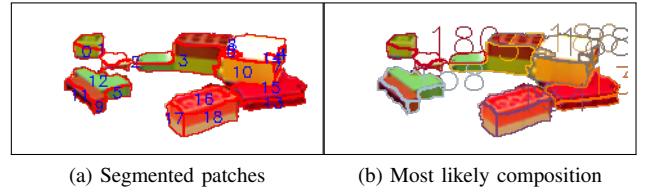


Fig. 8. “Best object” is able to move an object when “Best composition” fails. Time step 6 in the sixth scene in Fig. 6b: (a) Segmented patches, (b) the most likely object composition (probability 0.271). “Best object” grasps successfully an object hypothesis consisting of patches 0 and 1. However, “Best composition” finishes because segments 0, 1, and 2 form in (b) object hypothesis 180, which can not be grasped.

objects (“POMDP”)

- POMDP multi-step planning with hallucinating hidden objects (“POMDP with hallucination”)

The first two methods are similar to the ones used in table clearing in Section VI-B. The “POMDP” method uses a dynamics and observation model and using the model and the probability distribution based sufficient statistic plans multi-step actions as described in Section V. The “POMDP with hallucination” method extends the third method with a probability model for hidden objects as defined in Section IV-D while the probability for hidden objects to be red was estimated as the average fraction of visible red objects linearly scaled into $[0.2, 0.8]$ to always allow for both non-red and red hidden objects.

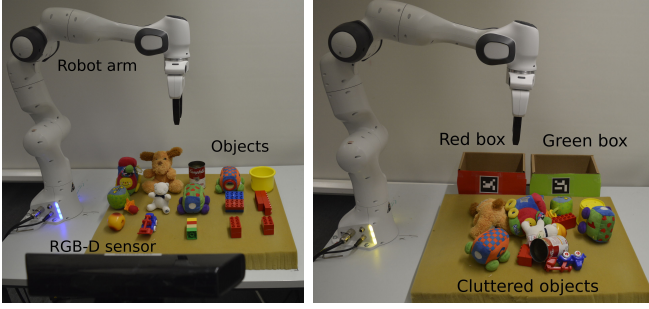


Fig. 9. Experimental setup for object search. Based on RGB-D data from a Microsoft Kinect, a 7-DOF Franka Panda robotic arm tries to move red objects into a red box. **(Left)** Robotic setup with all objects arranged on the table. **(Right)** In actual experiments, objects are dumped into the workspace resulting in a cluttered scene. The robot tries to move fully red objects into the red box and may put objects into the green box to reduce clutter.

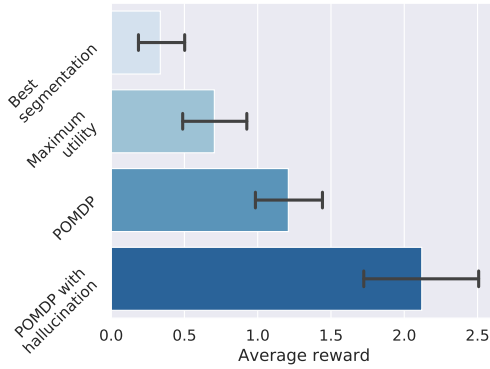


Fig. 10. Simulated object search. The bar plot shows the average reward and the 95% confidence interval for each method. The differences between the method performances is statistically significant. Please, see the main text for further discussion.

1) *Object Search with Simulated Dynamics.*: In object search simulation experiments, we used the initial RGB-D scenes captured in the robot experiments discussed in Section VI-C2 but simulated dynamics and observation probabilities. Fig. 10 shows the results. For statistical analysis we ran a Kruskal-Wallis test and then Posthoc Conover tests revealing that all methods' average reward differed statistically significantly: "POMDP with hallucination" from "POMDP" ($p = 0.002$), "POMDP" from "Maximum utility" ($p = 0.003$), and "Maximum utility" from "Best segmentation" ($p = 0.021$).

2) *Object Search on Real Hardware.*: Fig. 9 shows the experimental setup and one of the scenes we used for object search with a Franka Panda robot. As in previous experiments, we randomly generated scenes by adding all objects into a box, shook the box, and emptied the content into the robot's workspace.

Fig. 12 summarizes the results: POMDP methods significantly outperformed the greedy approaches. The main reasons the POMDP methods outperform the greedy approaches is that they utilize information gathering actions and remove occluding non-red objects as shown in Fig. 11 and plan actions over distributions of compositions. Planning over a distribution of compositions discourages our approach from stopping

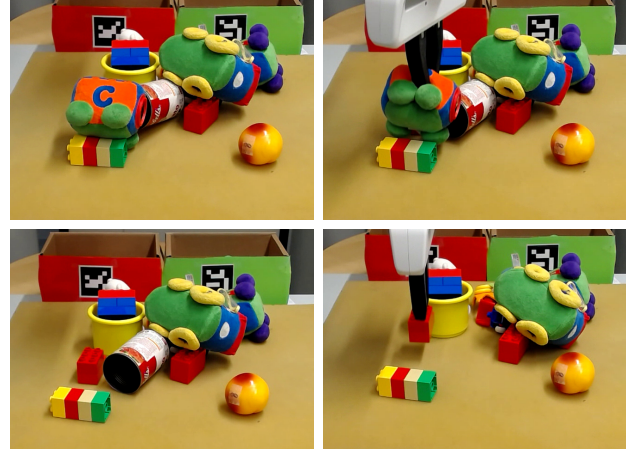


Fig. 11. The "POMDP with hallucination" method removes objects occluding a large space to reveal a fully red object. **(Upper Left)** Initial scene. **(Upper Right)** Picking up non-red object occluding a large space. **(Bottom Left)** A fully red hidden object is revealed. **(Bottom Right)** The robot now picks up the red object and moves it into the red box.

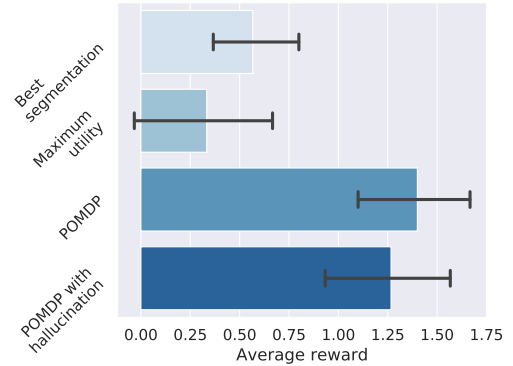


Fig. 12. Object search with a Franka Panda robot arm. The bar plot shows the average reward and the 95% confidence interval for each method. The performance difference between the POMDP methods and the greedy methods is statistically significant. Please, see the main text for further discussion.

prematurely, contrary to approaches that may stop when no red object is seen in the most probable distribution. Moreover, planning using a distribution of compositions enables complex reasoning such as moving a non-red object hypothesis away to verify whether it forms together with another red object hypothesis an object as shown in Fig. 13: if the hypotheses do not belong together we have removed a non-red object and can next collect the red object, while if the red and non-red hypotheses are part of the same object we still have removed only a non-red object and clarified the situation. Fig. 14 shows the running times for all comparison methods for the different computational components at different phases of the manipulation task.

"POMDP with hallucination" removed 21 occluding non-red objects to reveal a fully red object and "POMDP" 18 occluding non-red objects. Fig. 11 shows one successful example where "POMDP with hallucination" removes an obstacle to reveal a fully red object which is subsequently moved into the red box. We hypothesize that with bigger and/or more

occluding non-red objects or fewer red objects in total the performance of “POMDP with hallucination” may outperform the regular “POMDP” method as it has an inherent advantage of removing occluding objects in the scene.

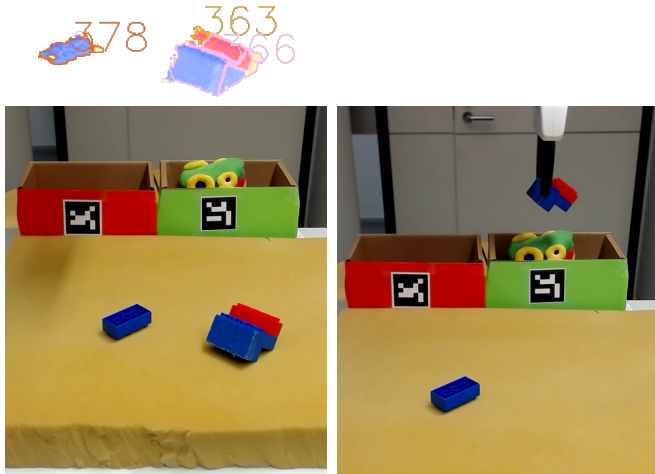


Fig. 13. **(Left)** The object composition on the top indicates that the red lego block is either separated or part of the larger blue object. A reasonable approach here is to grasp the larger blue part and move it to the green box. Then if the composition is separable the red lego will be left in the scene while if the red is part of the larger blue object the red-blue object will disappear which is also fine. **(Right)** Robot picked up the larger blue object. In this case the red segment was part of the blue object.

VII. CONCLUSIONS

Manipulating unknown objects in a cluttered environment is a hard but important problem in robotics. Allowing robots to operate in cluttered unknown environments is essential for robot autonomy and succeeding in tasks such as waste segregation, agile manufacturing, service robotics, and rescue robotics. However, a lack of object models and a noisy partial view make manipulation in such environments difficult. To

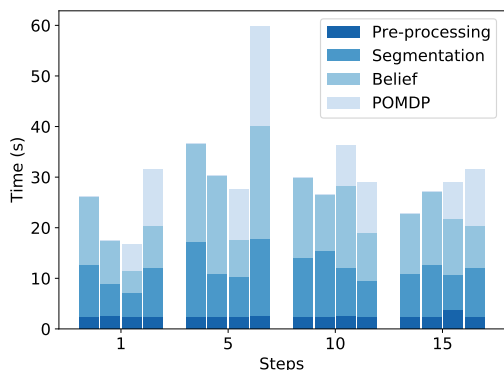


Fig. 14. The average running time for each comparison method at different phases of the manipulation task, that is, the time step. The running time is split into pre-processing, segmentation, belief generation, and the POMDP solver components. The four comparison methods are, from left to right, “Best segmentation”, “Maximum utility”, “POMDP” and “POMDP with hallucination”. Segmentation, belief generation, and the POMDP solver take roughly the same amount of processing time. This is by design since the running time of belief generation and the POMDP solver can be controlled while increasing or decreasing the exactness of the computations.

succeed in such tasks the robot needs to consider possible object compositions and in particular plan actions so that the actions chosen take all possible object compositions now and in future time steps into account. Therefore, instead of utilizing only the most likely object composition, we plan manipulation actions in the space of object compositions. In object search and table clearing experiments, our approach outperforms an approach based on the most likely object composition. Moreover, long term planning outperforms a greedy approach when planning over a distribution over object compositions.

In this paper we considered a setting with static objects. Future work includes manipulation of dynamic moving objects under occlusion. Moreover, our probabilistic world model allows for straightforward inclusion of prior knowledge when available and thus inclusion of different types of sensors such as tactile sensors is an avenue for future work. We expect the main idea of planning behavior based on a distribution of object compositions to transfer to many application domains. For example, in autonomous driving there can be high uncertainty due to occlusion and weather conditions: which parts of the scene are pedestrians?, which parts are cars?, which are buildings? Planning based on the distribution of object compositions is a safer alternative than relying on the most likely object composition which may be incorrect.

REFERENCES

- [1] J. Bohg, K. Hausman, B. Sankaran, O. Brock, D. Kragic, S. Schaal, and G. S. Sukhatme, “Interactive perception: Leveraging action in perception and perception in action,” *IEEE Transactions on Robotics*, vol. 33, no. 6, pp. 1273–1291, 2017.
- [2] J. Pajarinen and V. Kyrki, “Decision making under uncertain segmentations,” in *IEEE International Conference on Robotics and Automation (ICRA)*. IEEE, 2015, pp. 1303–1309.
- [3] —, “Robotic manipulation in object composition space,” in *IEEE/RSJ International Conference on Intelligent Robots and Systems (IROS)*. IEEE, 2014, pp. 1–6.
- [4] R. M. Haralick and L. G. Shapiro, “Image segmentation techniques,” *Computer vision, graphics, and image processing*, vol. 29, no. 1, pp. 100–132, 1985.
- [5] N. R. Pal and S. K. Pal, “A review on image segmentation techniques,” *Pattern recognition*, vol. 26, no. 9, pp. 1277–1294, 1993.
- [6] J. Shi and J. Malik, “Normalized cuts and image segmentation,” *IEEE Transactions on Pattern Analysis and Machine Intelligence*, vol. 22, no. 8, pp. 888–905, 2000.
- [7] P. F. Felzenszwalb and D. P. Huttenlocher, “Efficient graph-based image segmentation,” *International Journal of Computer Vision*, vol. 59, no. 2, pp. 167–181, 2004.
- [8] A. Richtsfeld, T. Mörwald, J. Prankl, M. Zillich, and M. Vincze, “Learning of perceptual grouping for object segmentation on RGB-D data,” *Journal of visual communication and image representation*, vol. 25, no. 1, pp. 64–73, 2014.
- [9] K. Lai, L. Bo, X. Ren, and D. Fox, “A large-scale hierarchical multi-view RGB-D object dataset,” in *Proceedings of the IEEE International Conference on Robotics and Automation (ICRA)*. IEEE, 2011, pp. 1817–1824.
- [10] A. K. Mishra, A. Shrivastava, and Y. Aloimonos, “Segmenting “simple” objects using RGB-D,” in *Proceedings of the IEEE International Conference on Robotics and Automation (ICRA)*. IEEE, 2012, pp. 4406–4413.
- [11] A. Richtsfeld, T. Mörwald, J. Prankl, M. Zillich, and M. Vincze, “Segmentation of unknown objects in indoor environments,” in *Proceedings of the IEEE/RSJ International Conference on Intelligent Robots and Systems (IROS)*. IEEE, 2012, pp. 4791–4796.
- [12] M. Danielczuk, M. Matl, S. Gupta, A. Li, A. Lee, J. Mahler, and K. Goldberg, “Segmenting unknown 3d objects from real depth images using mask r-cnn trained on synthetic data,” in *International Conference on Robotics and Automation (ICRA)*. IEEE, 2019, pp. 7283–7290.

- [13] C. Xie, Y. Xiang, A. Mousavian, and D. Fox, "The best of both modes: Separately leveraging rgb and depth for unseen object instance segmentation," in *Conference on Robot Learning*, 2020, pp. 1369–1378.
- [14] D. Morrison, J. Leitner, and P. Corke, "Closing the loop for robotic grasping: A real-time, generative grasp synthesis approach," in *Proc. of Robotics: Science and Systems (RSS)*, 2018.
- [15] A. Mousavian, C. Eppner, and D. Fox, "6-dof grasnet: Variational grasp generation for object manipulation," in *Proceedings of the IEEE International Conference on Computer Vision*, 2019, pp. 2901–2910.
- [16] J. Mahler, J. Liang, S. Niyaz, M. Laskey, R. Doan, X. Liu, J. A. Ojea, and K. Goldberg, "Dex-net 2.0: Deep learning to plan robust grasps with synthetic point clouds and analytic grasp metrics," *arXiv preprint arXiv:1703.09312*, 2017.
- [17] J. Varley, C. DeChant, A. Richardson, J. Ruales, and P. Allen, "Shape completion enabled robotic grasping," in *IEEE/RSJ international conference on intelligent robots and systems (IROS)*. IEEE, 2017, pp. 2442–2447.
- [18] D. Beale, P. Irvani, and P. Hall, "Probabilistic models for robot-based object segmentation," *Robotics and Autonomous Systems*, vol. 59, no. 12, pp. 1080–1089, 2011.
- [19] H. van Hoof, O. Kroemer, and J. Peters, "Probabilistic segmentation and targeted exploration of objects in cluttered environments," *IEEE Transactions on Robotics*, vol. 30, no. 5, pp. 1198–1209, 2014.
- [20] D. Katz, M. Kazemi, J. Bagnell, and A. Stentz, "Clearing a pile of unknown objects using interactive perception," in *Proc. of IEEE International Conference on Robotics and Automation (ICRA)*, 2013, pp. 154–161.
- [21] Y. Y. Boykov and M.-P. Jolly, "Interactive graph cuts for optimal boundary & region segmentation of objects in ND images," in *Proceedings of the IEEE International Conference on Computer Vision (ICCV)*, vol. 1. IEEE, 2001, pp. 105–112.
- [22] T. Zhao and R. Nevatia, "Bayesian human segmentation in crowded situations," in *Proceedings of the IEEE Computer Society Conference on Computer Vision and Pattern Recognition (CVPR)*, vol. 2. IEEE, 2003.
- [23] Z. Tu and S. Zhu, "Image segmentation by data-driven Markov chain Monte Carlo," *IEEE Transactions on Pattern Analysis and Machine Intelligence*, vol. 24, no. 5, pp. 657–673, 2002.
- [24] Y. Yakimovsky, "Boundary and object detection in real world images," *Journal of the ACM (JACM)*, vol. 23, no. 4, pp. 599–618, 1976.
- [25] J. Redmon, S. Divvala, R. Girshick, and A. Farhadi, "You only look once: Unified, real-time object detection," in *Proceedings of the IEEE conference on computer vision and pattern recognition (CVPR)*, 2016, pp. 779–788.
- [26] H. Koppula, A. Anand, T. Joachims, and A. Saxena, "Semantic labeling of 3d point clouds for indoor scenes," in *Advances in Neural Information Processing Systems (NIPS)*, 2011, pp. 244–252.
- [27] A. Karpathy, S. Miller, and L. Fei-Fei, "Object discovery in 3D scenes via shape analysis," in *Proc. of IEEE International Conference on Robotics and Automation (ICRA)*. IEEE, 2013, pp. 2088–2095.
- [28] R. Bajcsy, "Active perception," *Proceedings of the IEEE*, vol. 76, no. 8, pp. 966–1005, 1988.
- [29] M. Bjorkman and D. Kragic, "Active 3D scene segmentation and detection of unknown objects," in *Proc. of IEEE International Conference on Robotics and Automation (ICRA)*. IEEE, 2010, pp. 3114–3120.
- [30] L. Chang, J. Smith, and D. Fox, "Interactive singulation of objects from a pile," in *Proc. of IEEE International Conference on Robotics and Automation (ICRA)*. IEEE, 2012, pp. 3875–3882.
- [31] H. Van Hoof, O. Kroemer, and J. Peters, "Probabilistic segmentation and targeted exploration of objects in cluttered environments," *IEEE Transactions on Robotics*, vol. 30, no. 5, pp. 1198–1209, 2014.
- [32] A. Saxena, J. Driemeyer, J. Kearns, and A. Ng, "Robotic grasping of novel objects," in *Advances in Neural Information Processing Systems (NIPS)*, 2006, pp. 1209–1216.
- [33] I. Lenz, H. Lee, and A. Saxena, "Deep learning for detecting robotic grasps," in *Proc. of Robotics: Science and Systems (RSS)*, 2013.
- [34] V. Satish, J. Mahler, and K. Goldberg, "On-policy dataset synthesis for learning robot grasping policies using fully convolutional deep networks," *IEEE Robotics and Automation Letters*, vol. 4, no. 2, pp. 1357–1364, 2019.
- [35] Y. Qin, R. Chen, H. Zhu, M. Song, J. Xu, and H. Su, "S4g: Amodal single-view single-shot se (3) grasp detection in cluttered scenes," in *Conference on Robot Learning*, 2020, pp. 53–65.
- [36] J. Mahler, M. Matl, V. Satish, M. Danielczuk, B. DeRose, S. McKinley, and K. Goldberg, "Learning ambidextrous robot grasping policies," *Science Robotics*, vol. 4, no. 26, 2019.
- [37] M. Dogar and S. Srinivasa, "A planning framework for non-prehensile manipulation under clutter and uncertainty," *Autonomous Robots*, vol. 33, no. 3, pp. 217–236, 2012.
- [38] K. Hsiao, L. P. Kaelbling, and T. Lozano-Perez, "Grasping POMDPs," in *Proc. of IEEE International Conference on Robotics and Automation (ICRA)*. IEEE, 2007, pp. 4685–4692.
- [39] K. Hsiao, L. P. Kaelbling, and T. Lozano-Pérez, "Robust grasping under object pose uncertainty," *Autonomous Robots*, vol. 31, no. 2-3, pp. 253–268, 2011.
- [40] J. Laaksonen, E. Nikandrova, and V. Kyrki, "Probabilistic sensor-based grasping," in *Proc. of IEEE/RSJ International Conference on Intelligent Robots and Systems (IROS)*, 2012, pp. 2019–2026.
- [41] E. Nikandrova, J. Laaksonen, and V. Kyrki, "Towards informative sensor-based grasp planning," *Robotics and Autonomous Systems*, vol. 62, no. 3, pp. 340–354, 2014.
- [42] P. Monso, G. Alenya, and C. Torras, "POMDP approach to robotized clothes separation," in *Proc. of IEEE/RSJ International Conference on Intelligent Robots and Systems (IROS)*. IEEE, 2012, pp. 1324–1329.
- [43] J. K. Li, D. Hsu, and W. S. Lee, "Act to see and see to act: POMDP planning for objects search in clutter," in *IEEE/RSJ International Conference on Intelligent Robots and Systems (IROS)*. IEEE, 2016, pp. 5701–5707.
- [44] Y. Xiao, S. Katt, A. ten Pas, S. Chen, and C. Amato, "Online planning for target object search in clutter under partial observability," in *International Conference on Robotics and Automation (ICRA)*. IEEE, 2019, pp. 8241–8247.
- [45] D. Fischinger, M. Vincze, and Y. Jiang, "Learning grasps for unknown objects in cluttered scenes," in *Proc. of IEEE International Conference on Robotics and Automation (ICRA)*. IEEE, 2013, pp. 609–616.
- [46] S. Koenig and R. Simmons, *Xavier: A robot navigation architecture based on partially observable Markov decision process models*. MIT Press, 1998, pp. 91–122.
- [47] H. Bai, S. Cai, N. Ye, D. Hsu, and W. S. Lee, "Intention-aware online POMDP planning for autonomous driving in a crowd," in *IEEE International Conference on Robotics and Automation (ICRA)*. IEEE, 2015, pp. 454–460.
- [48] T. Taha, J. V. Miró, and G. Dissanayake, "A POMDP framework for modelling human interaction with assistive robots," in *IEEE International Conference on Robotics and Automation (ICRA)*. IEEE, 2011, pp. 544–549.
- [49] J. Pajarinen and V. Kyrki, "Robotic manipulation of multiple objects as a POMDP," *Artificial Intelligence*, vol. 247, pp. 213–228, 2017.
- [50] J. Pajarinen, "Technical report: The policy graph improvement algorithm," Aalto University, Tech. Rep., 2020. [Online]. Available: <https://arxiv.org/abs/2009.02164>
- [51] G. Casella and E. I. George, "Explaining the Gibbs sampler," *The American Statistician*, vol. 46, no. 3, pp. 167–174, 1992.
- [52] D. J. C. MacKay, *Information theory, inference and learning algorithms*. Cambridge university press, 2003.
- [53] D. A. Levin, Y. Peres, and E. L. Wilmer, *Markov chains and mixing times*. American Mathematical Society, 2009.
- [54] J. G. Propp and D. B. Wilson, "Exact sampling with coupled Markov chains and applications to statistical mechanics," *Random structures and Algorithms*, vol. 9, no. 1-2, pp. 223–252, 1996.
- [55] O. Häggström and K. Nelander, "Exact sampling from anti-monotone systems," *Statistica Neerlandica*, vol. 52, no. 3, pp. 360–380, 1998.
- [56] A. Gelman, J. B. Carlin, H. S. Stern, D. B. Dunson, A. Vehtari, and D. B. Rubin, *Bayesian data analysis*. CRC press, 2013.
- [57] H. B. Mann and D. R. Whitney, "On a test of whether one of two random variables is stochastically larger than the other," *The Annals of Mathematical Statistics*, vol. 18, no. 1, pp. 50–60, 1947.
- [58] M. Danielczuk, A. Angelova, V. Vanhoucke, and K. Goldberg, "X-ray: Mechanical search for an occluded object by minimizing support of learned occupancy distributions," *arXiv preprint arXiv:2004.09039*, 2020.